The winged helix transcription factor Foxg1 facilitates retinal ganglion cell axon crossing of the ventral midline in the mouse

Thomas Pratt*, Natasha M. M.-L. Tian, T. Ian Simpson, John O. Mason and David J. Price

Genes and Development Group, Biomedical Sciences, George Square, The University of Edinburgh, Edinburgh EH8 9XD, UK
*Author for correspondence (e-mail: t.pratt@ed.ac.uk)

Accepted 27 April 2004

Development 131, 3773-3784
Published by The Company of Biologists 2004
doi:10.1242/dev.01246

Summary

During normal development, retinal ganglion cells (RGCs) project axons along the optic nerve to the optic chiasm on the ventral surface of the hypothalamus. In rodents, most RGC growth cones then cross the ventral midline to join the contralateral optic tract; those that do not cross join the ipsilateral optic tract. Contralaterally projecting RGCs are distributed across the retina whereas ipsilaterally projecting RGCs are concentrated in temporal retina. The transcription factor Foxg1 (also known as BF1) is expressed at several key locations along this pathway. Analysis of *Foxg1* expression using *lacZ* reporter transgenes shows that *Foxg1* is normally expressed in most, if not all, nasal RGCs but not in most temporal RGCs, neither at the time they project nor earlier in their lineage. Foxg1 is also expressed at the optic chiasm. Mice that lack Foxg1 die at birth and, although the shape of their eyes is abnormal, their retinas still project axons to the brain via the optic chiasm. Using anterograde and retrograde tract tracing, we show that there is an eightfold increase in the ipsilateral projection in *Foxg1*$^{-/-}$ embryos. The distributions of cells expressing the transcription factors Foxg1 and Nkx2.2, and cell-surface molecules Ephb2, ephrin B2 and SSEA-1 (Fut4) have been correlated to the normally developing retinothalamic projection and we show they are not much altered in the developing *Foxg1*$^{-/-}$ retina and optic chiasm. As much of the increased ipsilateral projection in *Foxg1*$^{-/-}$ embryos arises from temporal RGCs that are unlikely to have an autonomous requirement for Foxg1, we propose that the phenotype reflects at least in part a requirement for Foxg1 outwith the RGCs themselves, most likely at the optic chiasm.

Key words: Eye, BF1, Optic chiasm, Retinal ganglion cell axons, Ipsilateral, Contralateral, Ephb, Ephrin B, Tract tracing, Mouse

Introduction

During brain development, neurons project axons tipped with navigating growth cones. Ultimately, these axons reach and form synaptic connections with their target cells. Axon tracts connecting brain regions can be divided into two classes depending on whether they cross the midline. Ipsilateral (or longitudinal) tracts, such as the thalamocortical tract, connect regions on the same side of the brain. Contralateral (or commissural) tracts, such as the corpus callosum, cross the midline of the brain and connect regions in different halves. The visual system exhibits both types of tract. Each optic nerve carries RGC axons from the retina towards the optic chiasm on the ventral surface of the hypothalamus. At the optic chiasm some RGC axons progress contralaterally and others progress ipsilaterally to join the optic tract and grow towards their targets in the forebrain and midbrain. This way of organising retinal output results in parts of the brain receiving binocular input, which is useful for judging positions of objects in space.

The behaviour of a growth cone at a specific point along its route is defined by its interaction with the cells and molecules it encounters. In the mouse, RGC axons exit the retina and start to navigate along the optic stalk (forming the optic nerve) at embryonic day 11 (E11) (Colello and Guillery, 1990). By E15.5, the chiasm has acquired its mature configuration although progressively more axons navigate this route during subsequent development (Marcus et al., 1995). At the optic chiasm RGC growth cones respond to cues generated by a specialised population of midline cells (Wizenmann et al., 1993; Sretavan and Reichardt, 1993; Marcus et al., 1995). Their importance is shown by the failure of optic tract formation in mice with an immunoablated chiasm (Sretavan et al., 1995) and the development of only ipsilateral projections in *Pax2*$^{-/-}$ or *Vax1*$^{-/-}$ mice with agenesis of the chiasm (Torres et al., 1996; Hallonet et al., 1999). Contralaterally projecting RGCs (the majority in mice) are distributed all over the retinal surface. Ipsilaterally projecting RGCs are concentrated in ventrotemporal retina and their axons are repelled at the optic chiasm (Sretavan and Reichardt, 1993; Herrera et al., 2003; Williams et al., 2003).

Several transcription factors are regionally expressed in the developing visual system and are poised to regulate the development of its structures and axonal connections (Torres et al., 1996; Halonet et al., 1999; Barbieri et al., 2002; Mui et al., 2002; Wang et al., 2002; de Melo et al., 2003; Herrera et al., 2003). The winged helix transcription factor Foxg1 is strongly expressed in the developing nasal retina and optic stalk, optic chiasm, telencephalon and superior colliculus (Xuan et al., 1995; Huh et al., 1999; Marcus et al., 1999). The most obvious anatomical defects in embryos homozygous for a targeted deletion of *Foxg1* are abnormally shaped eyes and a hypoplastic telencephalon (Xuan et al., 1995; Huh et al., 1999).

We have shown by injecting tract-tracers into the eyes of these mutants that the retina projects axons to an optic tract growing over the surface of the thalamus (Pratt et al., 2002).

To test the potential for Foxg1 to influence axon navigation, we used carbocyanine dyes to trace retinal axons in mice carrying a targeted deletion of *Foxg1* (Xuan et al., 1995; Hebert and McConnell, 2000). We found that mice lacking Foxg1 have an increased ipsilateral projection arising from both nasal and temporal retina. To characterise this defect, we (1) used *lacZ* reporter transgenes to identify potential sites at which Foxg1 expression might influence the navigation of retinofugal axons; and (2) examined several molecular markers expressed in the normal retina and optic chiasm, namely the transcription factors Foxg1 and Nkx2.2, the receptor tyrosine kinase Ephb2 and its ligand ephrin B2, and the stage-specific embryonic antigen 1 (SSEA-1; Fut4 – Mouse Genome Informatics) (Marcus et al., 1999; Barbieri et al., 2002; Williams et al., 2003) in *Foxg1*$^{-/-}$ embryos.

Materials and methods

Foxg1 alleles and genetic background

To identify cells in which the *Foxg1* locus is transcriptionally active, we exploited the *Foxg1*^{tm1M} (or *Foxg1*^{lacZ}) allele in which coding sequences are replaced by a *lacZ* cassette (Xuan et al., 1995). For tract tracing, we used the *Foxg1*$^{tm1(cre)Skm}$ (or *Foxg1*^{Cre}) allele in which coding sequences are replaced by a Cre recombinase cassette (Hebert and McConnell, 2000). *Foxg1*^{Cre} and *Foxg1*^{lacZ} are predicted null alleles (designated *Foxg1*$^{-}$) (Xuan et al., 1995; Hebert and McConnell, 2000). For lineage tracing, we used *Gtrosa26*^{tm1Sho} (*R26RS*) reporter mice (Mao et al., 1999). Cre-mediated recombination in *Foxg1*^{Cre};*R26RS* embryos irreversibly activates *lacZ* expression from the *ROSA26* locus (Mao et al., 1999; Hebert and McConnell, 2000). Tract tracing and lineage tracing experiments used the *Foxg1*^{Cre} allele on an albino Swiss Webster background (as described by Hebert and McConnell, 2000). Other experiments used *Foxg1*^{lacZ} and/or *Foxg1*^{Cre} alleles on a mixed pigmented CBA/C57Bl6/Swiss Webster background. *Foxg1* homozygous mutants (*Foxg1*$^{Cre/Cre}$) and compound heterozygotes (*Foxg1*$^{Cre/lacZ}$) were identified by their hypoplastic telencephalon and distorted eyes. Heterozygous embryos (i.e. *Foxg1*$^{+/-}$) were identified by PCR genotyping: they were indistinguishable morphologically from wild type (Xuan et al., 1995; Huh et al., 1999) and we detected no RGC axon projection defects at the optic chiasm (data not shown).

PCR genotyping *Foxg1* alleles

Foxg1^{+} was detected with primers Foxg1ORFFor 5′-CTG ACG CTC AAT GGC ATC TA-3′ and Foxg1ORFRev 5′-TTT GAG TCA ACA CGG AGC TG-3′ which give a product of 438 bp; *Foxg1*^{lacZ} allele was detected with primers Foxg1_5′UTRF 5′-GCT GGA CAT GGG AGA TAG GA-3′ and Foxg1*lacZ*_ORFR 5′-GAC AGT ATC GGC CTC AGG AA-3′ which give a 550 bp product; *Foxg1*^{Cre} allele was detected with primers NLSCreF 5′-CAT TTG GGC CAG CTA AAC AT-3′; NLSCreR 5′-ATT CTC CCA CCG TCA GTAC G-3′, which give a 307 bp product. For all primers, cycling conditions were 96°C for 2 minutes followed by [96°C for 30 seconds, 58.5°C for 30 seconds and 72°C for 30 seconds] for 35 cycles.

lacZ staining

E14.5 *Foxg1*$^{lacZ/+}$ and *Foxg1*$^{lacZ/Cre}$ embryonic heads were dissected and fixed for 1 hour at 4°C in 4% paraformaldehyde, 0.02% NP40, 0.01% sodium deoxycholate, 5 mM EGTA, 2mM $MgCl_2$ in phosphate-buffered saline (PBS). In some cases, heads were equilibrated in 30% sucrose/PBS and sectioned (10 μm) on a cryostat. Tissues were rinsed several times in wash buffer (2 mM $MgCl_2$, 0.02% NP40, 0.01% sodium deoxycholate in PBS), transferred to staining solution (wash buffer supplemented with 5 mM potassium ferricyanide, 5 mM potassium ferrocyanide and 1 mg/ml X-gal), and stained overnight (cryostat sections on slides) or for 2 days with agitation (wholemounts) at 37°C in darkness. Staining was stopped with 20 mM EDTA in PBS. Some wholemounts were sectioned with a vibratome (200 μm) or processed to wax, sectioned (10 μm) and mounted. Cryostat sections were counterstained with Nuclear Fast Red.

Tract tracing

Embryos (E13.5) or heads (E15.5) were fixed at 4°C in 4% paraformaldehyde in PBS overnight. For retrograde labelling, the back of the head and tissues overlying the thalamus were removed, and small DiI or DiA crystals (Molecular Probes) were placed in a line over the dorsal thalamus on one side to ensure unilateral labelling of the optic tract. For anterograde labelling, the lens was removed and the optic cup packed with larger clumps of crystals. Embryos were returned to 4% paraformaldehyde in PBS in the dark at room temperature for about one month to allow tracers to diffuse along axons. Vibratome sections (200 μm) were cleared by sinking in 1:1 glycerol: PBS containing the nuclear counterstain TOPRO3 (0.2 μM, Molecular Probes) and then 9:1 glycerol:PBS. Sections were stored at 4°C. Images were acquired using an epifluorescence microscope and digital camera (Leica Microsystems, Germany) or a TCS NT confocal microscope (Leica Microsystems, Germany). For quantification DiI-labelled RGCs were assigned to either nasal or temporal retina (Fig. 1B,C,J,K) in serial horizontal sections (for examples of sections used, see Fig. 4). In epifluorescence (TRITC filter) images (Fig. 3A-J; Fig. 4D-F,K,L) DiI appears orange and TOPRO3 appears red and in confocal images (Fig. 3K,L; Fig. 4A-C,G-J,M-O) DiI appears red, DiA is green and TOPRO3 appears blue.

Immunohistochemistry

Ephb2 and ephrin B2 immunohistochemistry was performed as described (Batlle et al., 2002). Embryos (E13.5) or heads (E16.5) were fixed overnight in 4% paraformaldehyde in phosphate buffer high salt (PBHS) [0.04 M phosphate, 0.03 M NaCl (pH7.0)] at 4°C, processed to wax and sectioned (10 μm). After rehydration, endogenous peroxidase activity was blocked with 90% methanol:3% hydrogen peroxide. Antigens were unmasked by microwaving in 10 mM sodium citrate buffer (pH 6.0) before reacting overnight with primary antibody followed by a bridge rabbit anti-goat antibody and detection using the Envision^{+} (Rabbit) Kit (Dako K4010). Antibody incubation and pre-incubation blocking were carried out in 1% bovine serum albumin in PBS at room temperature. SSEA-1 and Nkx2.2 immunohistochemistry was performed as described [SSEA-1 (Marcus and Mason, 1995), Nkx2.2 (Pratt et al., 2000)] except that detection of the primary antibody was carried out using the Envision^{+} (Mouse) Kit (Dako K4006). Primary antibodies were goat anti-mouse ephrin B2 (R&D Systems AF496) used at 1:500; goat anti-mouse Ephb2 (R&D Systems AF467) used at 1:1000; rabbit anti-goat (Dako Z0228) used at 1:400; mouse monoclonal anti-Nkx2.2 antibody (DSHB, USA 74.5A5) used at 1:30; and mouse monoclonal anti-SSEA1 antibody (DSHB, USA MC-480) was used at 1:50. Following a diaminobenzidine colour reaction, sections were dehydrated and mounted.

Results

Foxg1 expression in the developing eye and chiasm at E14.5 in *Foxg1*$^{lacZ/+}$ and *Foxg1*$^{lacZ/Cre}$ embryos

To identify cells that express *Foxg1*, we took advantage of a ‘knock-in’ to the *Foxg1* locus in which a *lacZ* cassette replaces *Foxg1*-coding sequences and is expressed in cells transcriptionally activating the *Foxg1* locus. These cells are stained blue after incubation with X-gal solution (Fig. 1). If

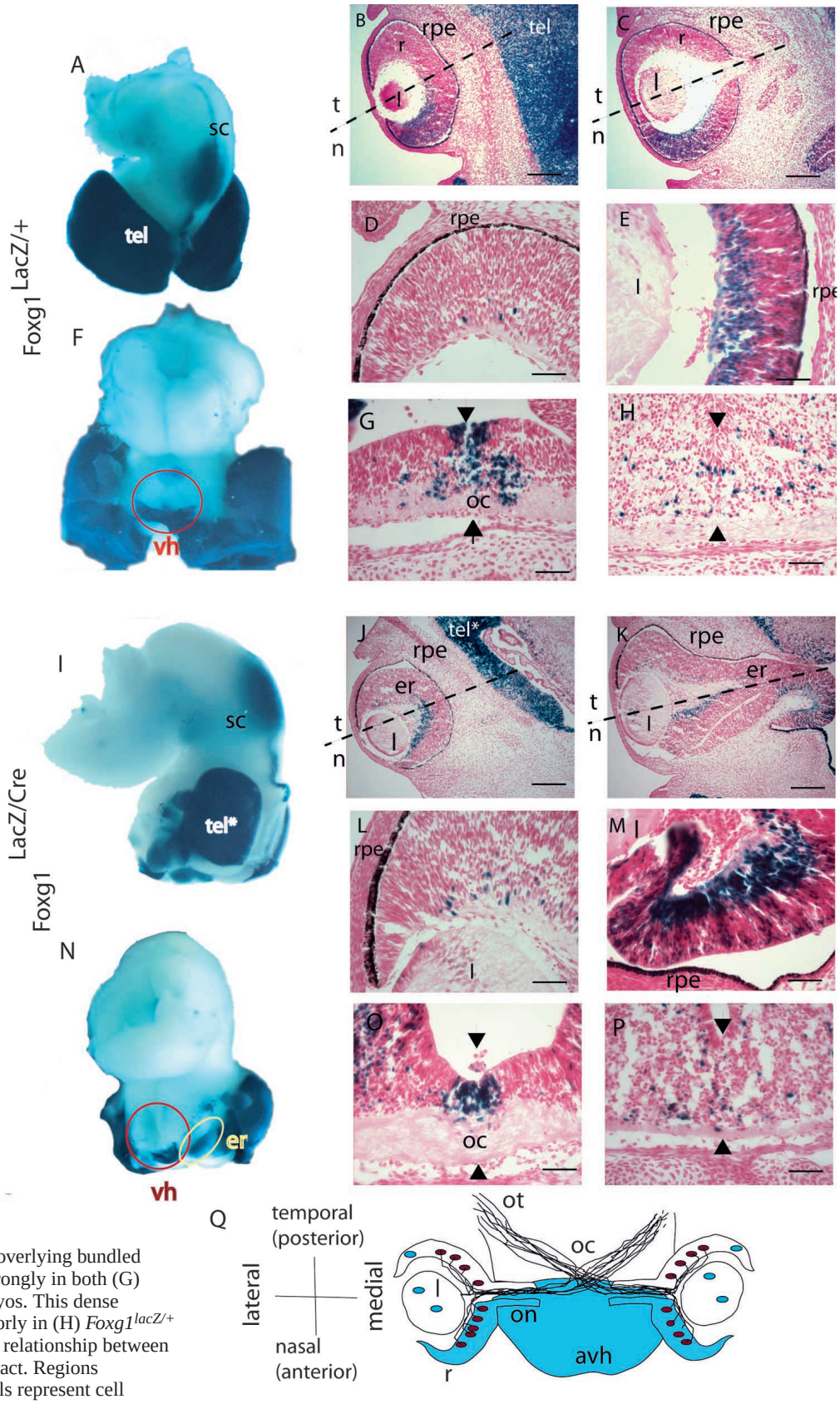

Fig. 1. Transcriptional activation of the *Foxg1* gene in tissues involved in RGC axon guidance in E14.5 embryos with and without Foxg1. *Foxg1*$^{lacZ/+}$ embryos have one functional copy of *Foxg1* and are phenotypically normal. *Foxg1*$^{lacZ/Cre}$ embryos are unable to produce Foxg1 protein. The *Foxg1*^{lacZ} allele reports transcriptional activation of the *Foxg1* gene by expression of *lacZ* protein. (A,F,I,N) X-gal stained brains. (A,F) *Foxg1*$^{lacZ/+}$ brain viewed (A) dorsolaterally to show staining of the superior colliculus (sc), dorsal midline and telencephalon (tel). (F) Ventral view shows staining in the anterior part of the ventral hypothalamus (vh; circled in red). (I,N) *Foxg1*$^{lacZ/Cre}$ brain showing (I) staining in the superior colliculus, along the dorsal midline and in the hypoplastic telencephalon (tel*). (N) A ventral view shows that, as in *Foxg1*$^{lacZ/+}$ embryos, staining is restricted to anterior ventral hypothalamus. The yellow oval encloses the mutant elongated retina (er), which has remained attached to the brain. The retinal pigment epithelium (rpe) has been removed to show that *lacZ* staining is far stronger in the anterior (nasal) retina. (B-E,G,H,J-M,O,P) X-gal stained cryostat sections with nuclei stained red. (B-E,J-M) Sections through the eye. Both (B-E) *Foxg1*$^{lacZ/+}$ and (J-M) *Foxg1*$^{lacZ/Cre}$ retinas exhibit predominantly nasal (n) *lacZ* staining, although in both cases a few stained cells are also detected in temporal (t) retina. J is dorsal to K. (K) Nasal staining in the medial elongation of the mutant retina. B and J are dorsal to D and K, respectively. (D,E,L,M) Higher magnifications of *Foxg1*$^{lacZ/+}$ and *Foxg1*$^{lacZ/Cre}$ (D,L) temporal and (E,M) nasal retina, showing pronounced staining of the nasal RGC layer. (G,H,O,P) Sections through the ventral hypothalamus with paired arrows demarcating its midline. A population of midline cells overlying bundled axons at the optic chiasm (oc) stains strongly in both (G) *Foxg1*$^{lacZ/+}$ and (O) *Foxg1*$^{lacZ/Cre}$ embryos. This dense midline staining is absent more posteriorly in (H) *Foxg1*$^{lacZ/+}$ and (P) *Foxg1*$^{lacZ/Cre}$ embryos. (Q) The relationship between Foxg1 expression and the retinofugal tract. Regions expressing Foxg1 are shaded blue. Ovals represent cell bodies. The retinofugal tract comprises RGCs (red) projecting axons (black lines) towards the optic chasm and into the brain. l, lens; ot, optic tract; r, retina; avh, anterior ventral hypothalamus; on, optic nerve. Wholemounts (A,F,I,N) are shown with anterior facing downwards. Cryostat sections (B-D,J-L) are horizontal with anterior (nasal) at the bottom; (E,G,H,M,O,P) coronal sections. Scale bars: 200 μm in B,C,J,K; 50 μm in D,EG,H,L,M,O,P.

these cells possess a functional *Foxg1* allele (i.e. in *Foxg1*$^{lacZ/+}$ embryos) they can make Foxg1 protein.

We examined *Foxg1* expression in *Foxg1*$^{lacZ/+}$ embryos at E14.5, because this is the time at which RGC axons are navigating the midline. *Foxg1* expression was strongest in the nasal retina (Fig. 1B,C); 51% of nasal cells were *lacZ*$^{+}$ in counts across several sections. By contrast, only a few temporal cells were lacZ^{+} (2%) (visible at higher magnifications in Fig. 1D). These findings are consistent with previous results of in situ hybridisation (Hatini et al., 1994). In the centronasal retina, staining was particularly prominent in the inner layer occupied by the RGCs (Fig. 1E). Foxg1 was expressed in the anterior hypothalamus (Fig. 1F) with a population of expressing cells at the ventral midline overlying bundled axons at the optic chiasm (Fig. 1G,H). Foxg1 was also expressed by other structures encountered (or avoided) by RGC axons, including the telencephalon, dorsal midline and superior colliculus (Fig. 1A).

We examined *lacZ* expression in *Foxg1*$^{lacZ/Cre}$ compound heterozygotes, which can produce no functional Foxg1 protein, so as to identify cells in which the mutant gene was transcriptionally activated at E14.5. As *Foxg1*$^{lacZ/Cre}$ cells had the same *lacZ* gene dose as *Foxg1*$^{lacZ/+}$ cells (one copy), *lacZ* staining intensity could be directly compared between the two genotypes. The *Foxg1*$^{-/-}$ eye is distorted (Fig. 1J,K) with an abnormally small lens and a medially elongated retina that extends towards the optic chiasm. The nasal bias of *Foxg1* expression in *Foxg1*$^{lacZ/+}$ embryos described above was also apparent in *Foxg1*$^{lacZ/Cre}$ embryos (see whole mount in Fig. 1N and sectioned material in Fig. 1J-M). We counted 21% *lacZ*$^{+}$ cells in nasal retina compared with only 3% *lacZ*$^{+}$ cells in temporal retina. The reduced count nasally reflects the absence of *lacZ*$^{+}$ cells in outer layers of the Foxg1$^{lacZ/Cre}$ lateral retina (compare Fig. 1B,C with J,K). Previous work at a younger age, E12.5, also showed *lacZ* expression in the eyes of *Foxg1*$^{lacZ/lacZ}$ embryos confined mainly to the nasal region of the mutant retina (Huh et al., 1999). As in *Foxg1*$^{lacZ/+}$ embryos, *lacZ* staining was prominent in the inner layer of the nasal retina (compare Fig. 1J-M with B-E). These data show that the nasotemporal polarity of the retina is maintained in *Foxg1*$^{-/-}$ mutants until at least E14.5; this conclusion is further supported by data presented later.

In E14.5 *Foxg1*$^{lacZ/Cre}$ compound heterozygotes, the anterior hypothalamus continued to express *Foxg1* around the ventral midline at the point contacted by the expanded mutant retina (Fig. 1N). As in *Foxg1*$^{lacZ/+}$ embryos, stained cells were detected at the ventral midline (Fig. 1O,P) indicating that Foxg1 is not required for the maintenance of this population of cells at the optic chiasm. *lacZ* staining was also retained in the telencephalon, along the dorsal midline and in the superior colliculus (Fig. 1I).

Lineage tracing of retinal cells that have expressed *Foxg1*

The experiments described above show that *Foxg1* is expressed by many nasal RGCs at the time their growth cones are navigating the chiasm. The few expressing cells we detected in the temporal retina were near to the lateral lip (or ciliary margin) of the temporal retina where progenitor cells proliferate (Perron et al., 1998; Zuber et al., 2003). It was therefore possible that Foxg1-expressing progenitors might populate the temporal retina with RGCs, the navigational responses of which were influenced by transient expression of Foxg1 earlier in their lineage. Crossing *Foxg1*$^{Cre/+}$ mice with *R26RS* reporter mice generates embryos in which a Cre recombinase-mediated recombination event irreversibly enables *lacZ* expression from the *Rosa26* locus in cells that express *Foxg1* (Mao et al., 1999; Hebert and McConnell, 2000). These cells and their descendants express *lacZ* protein, regardless of whether the *Foxg1* locus remains active. The *lacZ* expression pattern provides a convenient means of visualising cells whose fate may have been influenced by autonomous exposure to Foxg1.

As expected, the nasal retina of *Foxg1*$^{Cre/+}$*; R26RS* embryos exhibited uniform *lacZ* staining (Fig. 2A-D). Strong staining was also seen in lens, optic nerve and at the optic chiasm. In

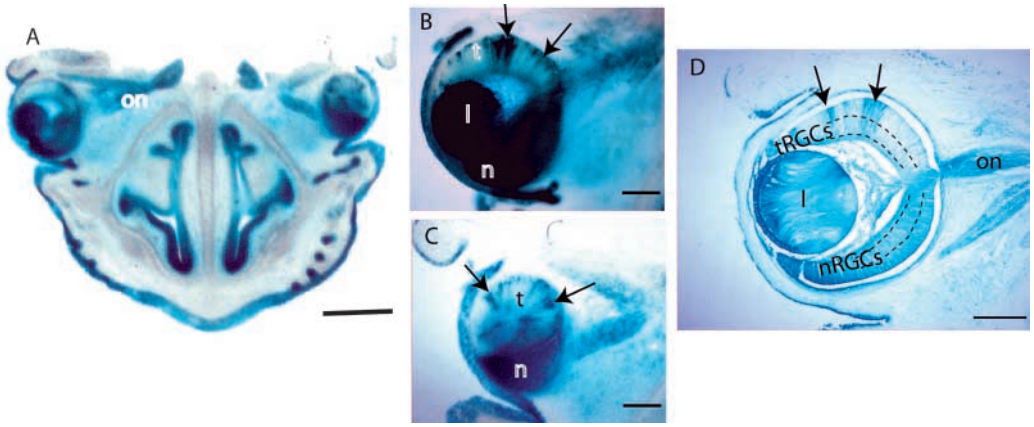

Fig. 2. Lineage tracing of *Foxg1*-expressing cells in E14.5 *Foxg1*$^{Cre/+}$*; R26RS* embryos. (A) Thick horizontal section of X-gal-stained facial whole mount (the eye on the right is sectioned more ventrally). *lacZ* staining is uniformly intense throughout the lens (l) and nasal (n) retina but appears patchy in the temporal (t) retina. (B,C) Thick horizontal sections of the eye. (B) Medial section; (C) ventral retina. (D) Thin horizontal section through the eye showing the distribution of *lacZ*-stained cells. Broken lines demarcate the position occupied by nasal RGCs (nRGCs) and temporal RGCs (tRGCs). In the nasal retina, *lacZ* staining is uniformly strong. In the temporal retina radial columns of *lacZ*-expressing cells are embedded in larger areas of non-expressing cells. In B and D, these columns are viewed side-on and in C they are viewed from above. Arrows in B-D indicate examples of *lacZ*-stained radial stripes. on, optic nerve. Scale bars: 500 μm in A; 200 μm in B-D.

the temporal retina of *Foxg1*$^{Cre/+}$*; R26RS* embryos, *lacZ* stained cells were found in radial stripes most of which were one or two cells wide while others were wider (Fig. 2B-D; arrows indicate radial stripes in temporal retina). A similar stripy distribution has been described before in chimeras and arises because the retina is constructed from radially oriented clones of cells (Reese et al., 1999). Examination of serial sections though the eyes of six embryos did not reveal any clear pattern in the size or density of these radial stripes, implying that the exposure of their ancestors to Foxg1 did not predispose them to occupy any particular part of the temporal retina. It was also apparent that most temporal RGCs were located outside the *lacZ*-expressing clones. These *lacZ*-expressing clones included cells outside the RGC layer showing that ancestral *Foxg1* expression was not restricted to RGCs. We also detected mosaic activation of *lacZ* expression in the temporal retinal pigment epithelium (a derivative of the optic cup, as is the retina) suggesting that a subpopulation of these cells are derived from Foxg1-expressing cells.

In conclusion, nasal RGCs express Foxg1 at the time their axons are negotiating the optic chiasm. By contrast, although some temporal RGCs are descended from Foxg1-expressing precursors, the vast majority do not express Foxg1 at this time and have never expressed Foxg1 at any time in their lineage.

Disruption to RGC axon navigation in embryos lacking Foxg1

The polarisation of *Foxg1* expression in the retina suggests that it could play an autonomous role in the navigation of nasal RGC growth cones but is unlikely to play an autonomous role in the navigation of most temporal RGC growth cones. Foxg1 may, however, influence the navigation of both nasal and temporal RGC growth cones by regulating the properties of the optic chiasm. To test these possibilities, we used DiI and DiA to trace the RGC projections in embryos lacking Foxg1.

We examined RGC projections in wild type at E13.5 (Fig. 3A-C) and E15.5 (Fig. 3F-H), over which period the optic chiasm develops its mature configuration. Progressing through the brain from rostral to caudal, sections show the injection in the eye (Fig. 3A,F), the optic nerve approaching the optic chiasm along the ventral surface of the brain (Fig. 3B,G) and the optic tract growing dorsally over the thalamus (Fig. 3C,H). At both ages, the contralateral optic tract is more strongly labelled, indicating that the majority of RGC axons cross the midline at the optic chiasm (Fig. 3C,H). Double labelling with DiI injected into one eye and DiA into the other illustrates the X-shape formed by RGC axons at the chiasm (Fig. 3K). Labelling of the optic tract is predominantly from the

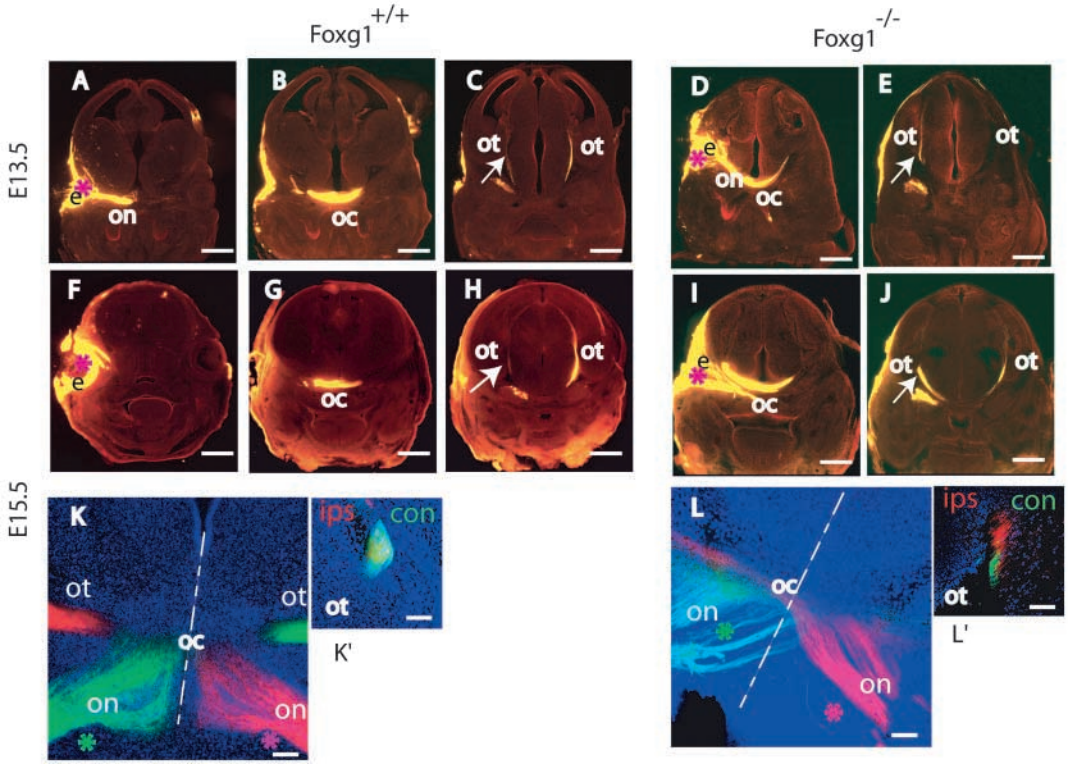

Fig. 3. RGC axon navigation in wild-type and *Foxg1*$^{-/-}$ embryos visualised by anterograde tract tracing at (A-E) E13.5 and (F-L) E15.5. For each age, progressively more caudal coronal sections of an individual embryo show injections of DiI (red asterisks) (A,F) in wild-type eye (e) and (D,I) in mutant eye; (B,G,D,I) labelling of optic nerve (on) and optic chiasm (oc); and (C,H,E,J) labelling of optic tracts (ot). (C,H) In the wild-type optic tracts, contralateral labelling is stronger than the ipsilateral labelling (white arrows). (E,J) In the mutant optic tracts, ipsilateral labelling appears stronger (white arrows). (K,L) Horizontal sections of embryos in which DiI was injected into one eye and DiA into the other eye of (K) an E15.5 wild-type and (L) an E15.5 *Foxg1*$^{-/-}$ embryo (ventral midline is marked by broken white line). (K′) Horizontal sections of the wild-type optic tract, growing over the diencephalon, from the same embryo as in K showing that each optic tract is predominantly labelled with dye from the contralateral (con) eye, although some ipsilateral (ips) label is also detectable (appears yellow where dyes overlap). (L′) Horizontal sections of the mutant optic tract from the same embryo as in L, showing abnormally high levels of red label from the ipsilateral eye. Scale bars: 500 μm in A-E; 650 μm in F-J; 100 μm in K,K′,L,L′.

contralateral eye, as shown by cross-sections of the optic tract as it grows dorsally over the thalamus (Fig. 3K′).

In E13.5 and E15.5 *Foxg1*$^{-/-}$ embryos many of the general features of RGC axon navigation were similar to those in wild type. RGC axons from both eyes converged on the ventral surface of the hypothalamus where they were sorted into ipsilateral and contralateral optic tracts growing dorsally over the thalamus (Fig. 3D,E,I,J). In contrast to the wild-type, the ipsilateral tract in mutants appeared greatly increased [compare panels for wild type (Fig. 3C,H) with mutants (Fig. 3E,J); arrows indicate the ipsilateral tract]. Double labelling with DiI injected into one eye and DiA into the other indicated that, although RGC axons converged at the hypothalamic midline, the balance of midline crossing was shifted in the mutants. Although many RGC axons still crossed the midline (Fig. 3L), a large proportion of axons in the optic tracts was labelled from the ipsilateral eye (Fig. 3L′).

To quantify the shift in the proportion of RGC axons projecting ipsilaterally and to identify the sites of origin in the retina of the aberrant ipsilateral projections, we retrogradely labelled RGCs with DiI or DiA from the thalamus. The numbers of nasal and temporal RGCs projecting ipsilaterally and contralaterally were counted in wild-type and mutant embryos at E15.5. As gene expression studies (Huh et al., 1999) (present study) indicate that, despite its medial elongation, the mutant retina does not exhibit greatly disturbed polarity, mutant eyes were divided into nasal and temporal halves using the same anatomical criteria as for wild-type eyes.

Wild-type embryos showed the expected patterns of projection. Retrograde label filled the optic tracts, optic chiasm and optic nerves, and showed most axons originating contralaterally (Fig. 4A-H). Contralaterally projecting RGCs were distributed across nasal and temporal retina (Fig. 4F,G). The much smaller number of ipsilaterally projecting RGCs were more frequently found temporally (Fig. 4G; Table 1). The density of labelled RGCs was highest medially, towards the optic nerve head, and decreased sharply in more lateral retina (Fig. 4F,G). RGC cell bodies were orientated radially with their axons projecting towards the optic nerve head along the inner surface of the retina (Fig. 4H).

In the mutant embryos, retrograde label filled the optic tracts, optic chiasm and optic nerves as in wild type (Fig. 4I-O) but many more axons originated ipsilaterally than in wild type [compare mutant (Fig. 4J) with wild type (Fig. 4C)]. This increased ipsilateral projection arose from both nasal and temporal retina (Fig. 4K,K′,M). Counts of ipsilateral RGCs in serial sections from four mutant and four wild-type E15.5 embryos (Table 1) showed an approximately eightfold increase in ipsilaterally projecting RGCs from both nasal and temporal retina in the mutants. There were no significant changes in the mutants in the numbers of RGCs projecting contralaterally from the nasal or temporal retina (Table 1). Total numbers of RGCs counted in the retina were not significantly altered in mutants. Ipsilaterally and contralaterally projecting RGCs were intermingled in the nasal and temporal retina (Fig. 4M, with higher magnification of RGCs in N) showing that all parts of the mutant retina contain RGCs capable of projecting to either side of the brain. We did not detect double-labelled cells, indicating that the increased ipsilateral projection did not result from large numbers of individual RGCs projecting to both sides of the brain.

As in the wild type, the majority of mutant RGCs are located in the inner layer of the retina and are radially orientated with their axons projecting along the inner surface of the retina (compare Fig. 4O with Fig. 4H), although the mutant RGCs do exhibit a broader radial spread. Again, reminiscent of the wild-type situation, mutant RGC axons fasciculate to form the mutant correlate of the optic nerve, which exits the elongated retina at its point of attachment to the ventral brain (seen in Fig. 4K) and approaches the optic chiasm (seen in a ventral adjacent section in Fig. 4L). As in the wild type, mutant retinal axons form an X-shaped chiasm (compare wild types in Fig. 3K, Fig. 4B,C,E with mutants in Fig. 3L, Fig. 4I,J,L), although their shapes are not identical. Given the distortions to the mutant eye it is remarkable that its retinal projection retains so many features in common with the wild type.

Our results in *Foxg1*$^{-/-}$ mutants indicate an increase in the proportion of RGCs whose axons are repelled by the midline and join the ipsilateral optic tract. As in wild type, significantly more ipsilateral projections originated in temporal retina (χ^2 test; Table 1). This finding provides further evidence for the retention of nasotemporal polarity, as was suggested by the expression pattern of *Foxg1* in mutants (see above).

Expression of Ephb2 and ephrin B2 in the developing retina

As well as being expressed in the developing retina itself, Foxg1 is expressed in cells that surround and may influence the patterns of expression of other genes in the retina as it develops (Dou et al., 1999). It was possible that in embryos lacking Foxg1 the patterning of the retina might have been altered fundamentally and this might have had consequences for RGC axon navigation. Results above suggested that the nasotemporal polarity of the *Foxg1*$^{-/-}$ retina is similar to wild type. Here, we addressed the nature of the other major axis of the mutant retina, i.e. dorsoventral. This was important as most ipsilateral RGC projections normally originate ventrally in the temporal retina (Drager, 1985) and so a repatterning of *Foxg1*$^{-/-}$ retina, such that it adopts a predominantly ventral character might have explained an increased ipsilateral projection.

The receptor tyrosine kinase Ephb2 and its ligand ephrin B2 are expressed in complementary dorsoventral gradients in the developing retina and their distributions in the retina and chiasm have been related to RGC axon midline crossing behaviour (Barbieri et al., 2002; Williams et al., 2003). In wild-type embryos at E13.5 and E16.5, ephrin B2 exhibits a dorsal$^{[high]}$ to ventral$^{[low]}$ gradient of expression in the retina with the strongest expression dorsolaterally (Fig. 5A,B). At E13.5, Ephb2 is expressed throughout the retina in a ventral$^{[high]}$ to dorsal$^{[low]}$ gradient (Fig. 5E). By E16.5 Ephb2 is more evenly distributed across the retina (Fig. 5F), although levels still appear to be slightly higher ventrolaterally. Ephb2 is also strongly expressed in the optic nerve, consistent with expression of Ephb2 protein on the RGC axons (Fig. 5E-F,I-J). RGC axons continue to express Ephb2 protein as they approach the optic chiasm and exit into the optic tract (Fig. 5I,J). By contrast, the optic nerve stains weakly for ephrin B2 protein (Fig. 5A,B).

The dorsoventral gradients of Ephb2 and ephrin B2 proteins are retained in the mutant. In E13.5 *Foxg1*$^{-/-}$ embryos, the retina expresses ephrin B2 protein in a dorsal$^{[high]}$ to

ventral[low] gradient (Fig. 5C) and Ephb2 protein in a complementary ventral[high] to dorsal[low] gradient (Fig. 5G). At E16.5, ephrin B2 expression is strongest in the dorsolateral retina (Fig. 5D) and Ephb2 protein is more evenly distributed across the retina with slightly higher levels ventrolaterally (Fig. 5H). As in wild types Ephb2 protein is expressed by mutant RGC axons as they cross the optic chiasm and enter the optic tracts (Fig. 5K,L).

In the wild type the eye is roughly spherical and is attached to the ventral surface of the diencephalon by the optic stalk, whereas the mutant eye lacks an optic stalk and is attached directly to brain. Perhaps as a mechanical consequence of this the mutant eye is elongated medially and squashed dorsoventrally relative to the wild-type eye. To distinguish whether this is only a change in shape or also involves a change in retinal volume, we measured retinal area (mm^2) in every 20th 10 μm horizontal serial section through the eyes of wild-type and mutant embryos. As each section was 0.01 mm thick, retinal volumes approximated to Σ(retinal area × 0.2) mm^3. Average volumes obtained for wild-type (0.86 mm^3) and mutant (0.88 mm^3) eyes were very similar. The proportion of the *Foxg1*$^{-/-}$ retina that is elongated medially (marked 'er' in Fig. 1K) probably corresponds to the central third of the wild-type retina. Consistent with this idea, the medial expansion of

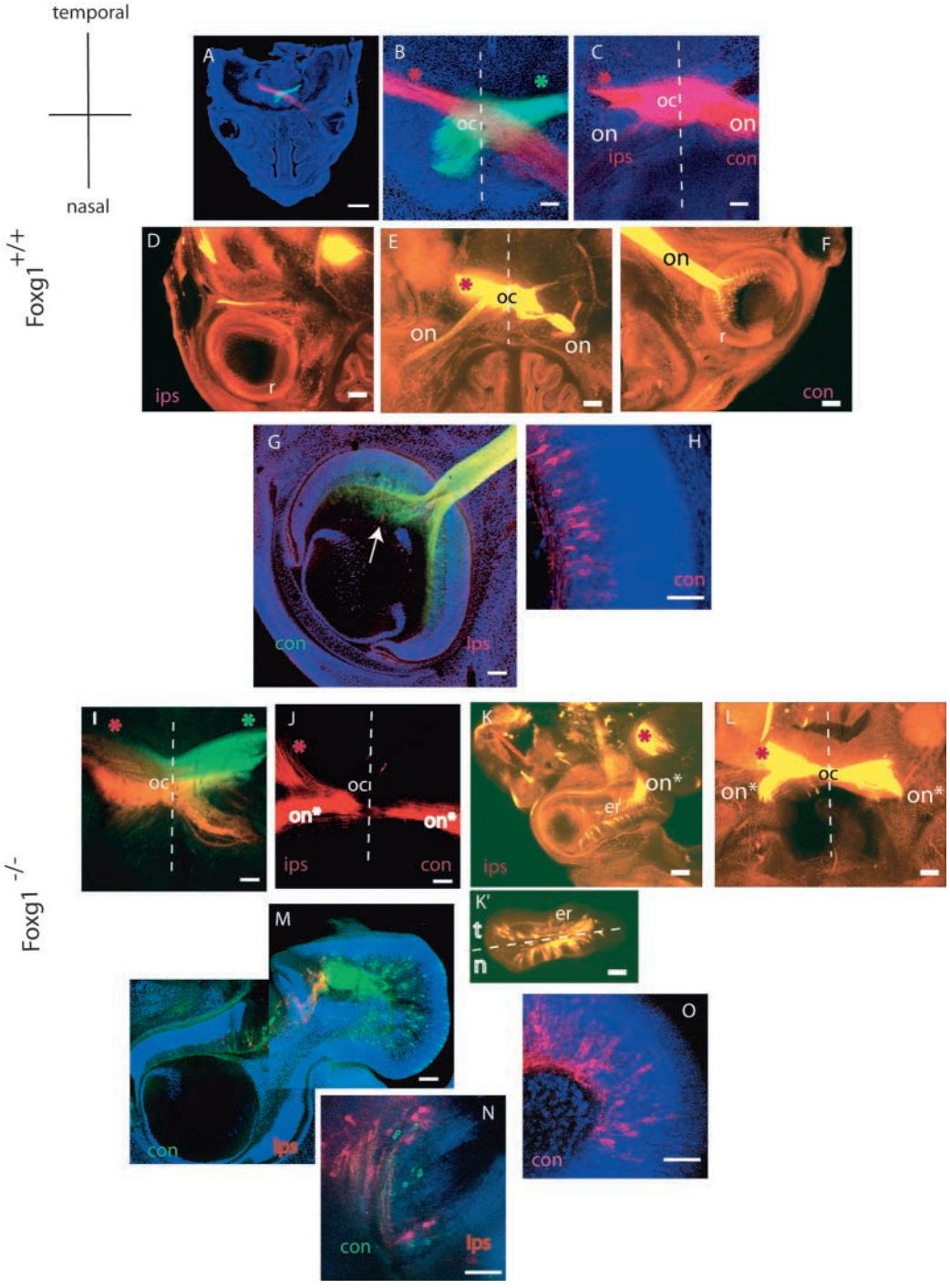

Fig. 4. Mapping ipsilateral and contralateral projecting RGCs in *Foxg1*$^{+/+}$ and *Foxg1*$^{Cre/Cre}$ embryos by retrograde tract tracing from the optic tract growing over the thalamus at E15.5. (A-H) Wild type. (A,B,G) DiI and DiA double-label experiment showing predominance of contralateral (con) projections (A,B) at the optic chiasm (oc) and (G) in the retina; an ipsilaterally (ips) labelled cell (red) is marked with arrow in G. (C-F,H) Single DiI-labelling experiments. (C,E) At the optic chiasm, the majority of labelling is in the contralateral optic nerve (on). (D,F) In the contralateral retina (F) a large number of labelled cells are distributed both nasally and temporally. (D) In the ipsilateral retina, far fewer cells are labelled. (I-O) Mutants. (I,M,N) Double-label experiment showing (I) the optic chiasm and (M,N) ipsilaterally (red) and contralaterally (green) projecting RGCs in the retina (note the absence of double labelled, yellow, RGCs). (J-L,O) Single label experiment showing increased ipsilateral labelling (compared with wild type) in (K,K′) both nasal (n) and temporal (t) parts of the elongated retina (er) and (J-L) their axons in the mutant correlate of the optic nerve (on*). (H,O) Higher magnification showing the disposition of RGCs in (H) wild-type and (O) mutant retina. All sections are horizontal with anterior (nasal) at the bottom. Each asterisk indicates which optic tract was injected with DiI (red) and DiA (green). Broken lines indicate the ventral midline. Scale bars: 500 μm in A; 100 μm in B,C,G,I,J,M; 200 μm in D-F,K,L; 50 μm in H,N,O.

Table 1. RGCs retrogradely labelled by dye placement in the optic tract

Midline crossing behaviour	Ipsilateral			Contralateral		
Hemiretina of origin	Temporal retina	Nasal retina	Temporal+ nasal retina	Temporal retina	Nasal retina	Temporal+ nasal retina
Foxg1$^{+/+}$ (*n*=4)	47	24	71	281	371	652
Foxg1$^{-/-}$ (*n*=4)	341	199	540	257	249	506
P values (*t*-test, *Foxg1*$^{+/+}$ versus *Foxg1*$^{-/-}$)	0.003*	0.021*	0.006*	0.84	0.48	0.6

Quantification of ipsilaterally and contralaterally projecting RGCs in nasal and temporal retina of *Foxg1*$^{+/+}$ and *Foxg1*$^{-/-}$ E15.5 embryos. DiI was injected into the optic tract on one side of the brain. After diffusion of DiI to the retina, serial horizontal sections were examined to determine: (1) the number of RGCs projecting to the injection site on the same side (ipsilateral) or opposite side (contralateral) of the brain; and (2) the number of RGCs of each class projecting from the nasal hemiretina or temporal hemiretina. Total RGC counts in serial sections from *Foxg1*$^{+/+}$ (*n*=4) and *Foxg1*$^{-/-}$ (*n*=4) embryos are tabulated. A χ^2 test was used to test the null hypothesis that nasal and temporal retina projected equal numbers of ipsilateral axons. The null hypothesis was rejected both for wild type (χ^2=3.73, *P*<0.05) and mutants (χ^2=18.6, *P*<0.05), indicating that both exhibited a significant temporal bias in the origin of ipsilateral projections. *P* values (Student's *t*-test) for *Foxg1*$^{+/+}$ versus *Foxg1*$^{-/-}$ comparison for each type of RGC counted are shown in the bottom row (*a significant difference).

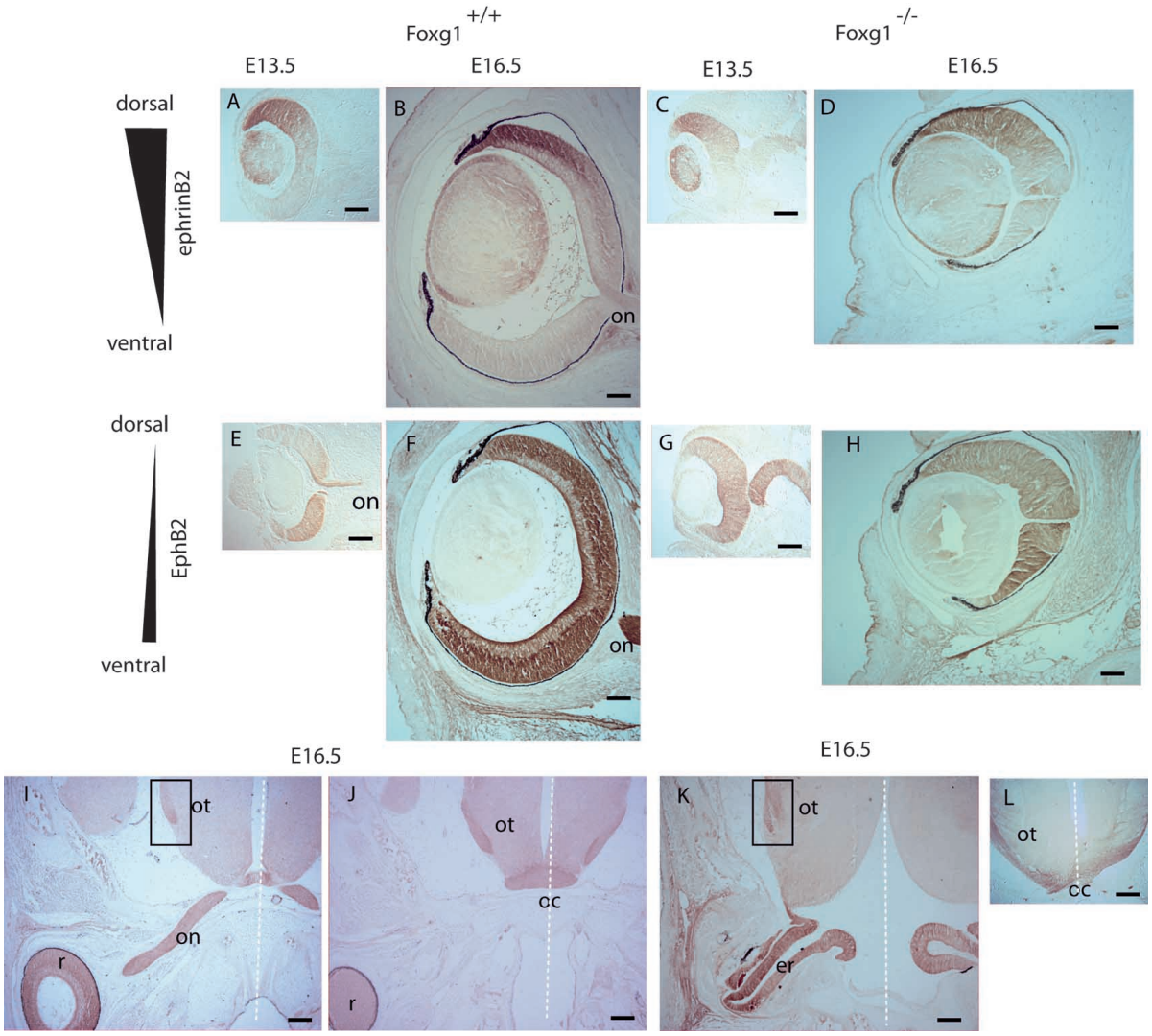

Fig. 5. The distributions of Ephb2 and ephrin B2 proteins in the developing retina and its axons are not dramatically altered in the *Foxg1*$^{-/-}$ mutant. Ephrin B2 protein forms a dorsolateral$^{[High]}$ to ventrolateral$^{[Low]}$ gradient in the developing retina at E13.5 in (A) the wild-type and (C) the mutant. This gradient remains at E16.5 in both (B) wild-type and (D) mutant. Ephb2 protein forms a complementary ventrolateral$^{[High]}$ to dorsolateral$^{[Low]}$ gradient in the developing retina at E13.5 in both (E) wild-type and (G) mutant retina. At E16.5, these gradients are shallower than at E13.5 in both (F) wild type and (H) mutant. The optic nerve (on) stains strongly for Ephb2 protein consistent with Ephb2 expression by navigating RGC axons. (I,J) In the wild type, Ephb2 is present in the optic nerve as it leaves the retina (r) and approaches the optic chiasm (oc) to emerge into the optic tract (ot) (boxed area in I). (K,L) In the mutant, Ephb2 is expressed in the elongated retina (er), at the optic chiasm and in the mutant optic tract as it emerges from the chiasm (boxed area in K). (A-H) Coronal sections (dorsal is towards the top); (I-L) horizontal sections (posterior is towards the top). Scale bars: 100 μm in A-H; 200 μm I-L.

the mutant retina expressed levels of ephrin B2 and Ephb2 intermediate between the extremes of the expression gradients shown in Fig. 5D,H (data not shown), as did the wild-type central retina.

These data indicate that, as in the nasotemporal axis, patterning of the retina along the dorsoventral axis is similar in *Foxg1*$^{-/-}$ and in wild-type embryos.

Expression of Nkx2.2, SSEA-1 and ephrin B2 at the developing chiasm

The presence of cells at the chiasm that turn on *Foxg1* in both *Foxg1*$^{+/+}$ and *Foxg1*$^{-/-}$ embryos (Fig. 1) prompted us to examine the mutant chiasm in more detail. The expression patterns of the transcription factor Nkx2.2 and the cell-surface molecule stage-specific embryonic antigen 1 (SSEA-1) define stages of normal chiasm development (Marcus and Mason, 1995; Marcus et al., 1999). SSEA-1 is expressed by a population of early differentiating neurons that provides an anatomical template to guide RGC axons at the developing chiasm (Sretavan et al., 1994; Marcus and Mason, 1995; Sretavan et al., 1995). We speculated that changes in the distribution of neurons expressing SSEA-1 in the mutant might perturb RGC axon midline crossing behaviour. However, we were unable to detect any clear shift in the expression domains of SSEA-1 between the wild-type (Fig. 7A,C,E) and mutant (Fig. 7B,D,F) chiasm at E13.5. The transcription factor Nkx2.2 defines a domain through which RGC axons grow at the midline (Marcus et al., 1999), but we did not find evidence of differences between Nkx2.2 expression in the wild-type and mutant (compare Fig. 7G with 7H). Ephrin B2 is expressed by radial glial cells that form a palisade at the chiasm and control RGC axon divergence (Marcus and Mason, 1995; Marcus et al., 1995; Nakagawa et al., 2000; Williams et al., 2003). Although the shape of the tissues surrounding the optic chiasm was slightly abnormal in *Foxg1* mutants, expression of ephrin B2 was observed along the ventral midline of the diencephalon in both wild-type and mutant embryos at E13.5 and E16.5 (Fig. 6). These data show that the mutant chiasm does not show major defects in the expression of at least three molecules known to be important for its interaction with RGC axons.

Discussion

Dual role for Foxg1 in eye morphogenesis and RGC axon guidance

During normal development, the eye field in the anterior neural plate splits into a right and a left half separated by the developing floor plate (reviewed by Rubenstein and Beachy, 1998; Rubenstein et al., 1998). On each side, the optic cup (from which retina and retinal pigment epithelium are derived) forms laterally, the optic stalk forms medially and the retina projects axons along the optic stalk to the chiasm. *Foxg1* is first expressed in the surface ectoderm immediately anterior to the neural plate at around E8 in mice. Over the following day, its expression appears in the anterior neural plate and, as this region becomes the anterior neural tube, demarcates the telencephalic neuroepithelium, optic chiasm and nasal retina (Hatini et al., 1994; Xuan et al., 1995; Dou et al., 1999; Huh et al., 1999). The domain of *Foxg1* expression in nasal retina includes the locations of projecting RGCs. Only a few cells in the temporal retina, which are located towards the ciliary margin, express *Foxg1*. Our data show that most RGCs in the temporal retina are descended from lineages in which *Foxg1* has never been expressed. These expression patterns indicate that Foxg1 is unlikely to have a significant cell autonomous effect on the development of cells in temporal retina, but may have such an effect on cells in nasal retina.

Our results show that Foxg1 is required to ensure a normal ipsilateral projection from RGCs. The *Foxg1*$^{-/-}$ retina produces an increased ipsilateral projection, arising from RGCs located

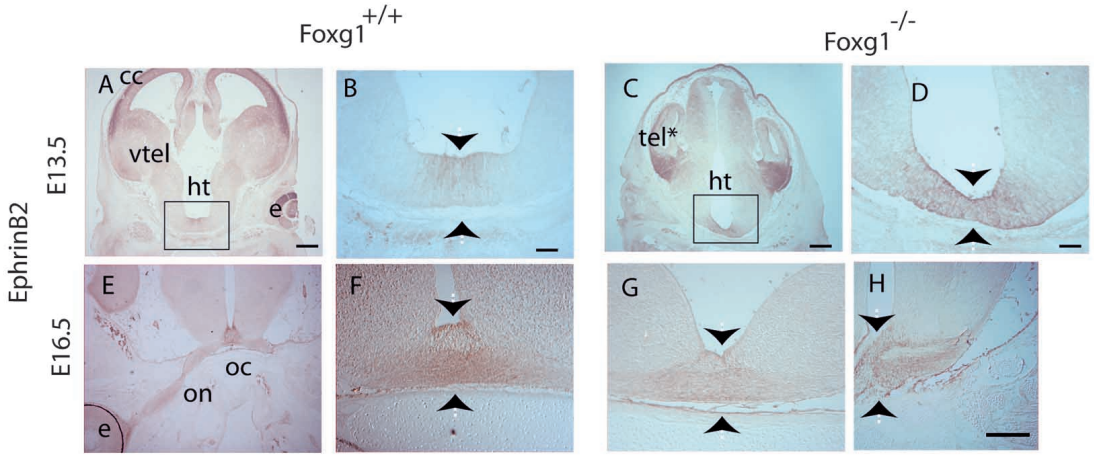

Fig. 6. Ephrin B2 protein is expressed at the ventral hypothalamic midline in both the *Foxg1*$^{-/-}$ mutant and the wild type. (A,B,E,F) Wild type. (A,B) At E13.5, ephrin B2 expression is most widespread in the more dorsal structures in the developing forebrain and eye (e). Ventrally ephrin B2 is detected at the ventral hypothalamic (ht) midline (B shows area boxed in A at higher power). (E,F) At E16.5, ephrin B2 protein is detected at the optic chiasm (oc) where expressing cells contact the optic nerve (on). (F) Higher magnification of the optic chiasm. (C,D,G,H) Mutant. (C,D) At E13.5, ephrin B2 is expressed in the hypoplastic telencephalon (tel*) and in the developing eye (see Fig. 5). Ephrin B2 is also detected at the hypothalamic midline (D shows area boxed in C at higher power). (G,H) At E16.5 ephrin B2 expression persists at the mutant optic chiasm where it contacts Ephb2-expressing axons (section in H is adjacent to the Ephb2 stained section shown in Fig. 5L). Paired arrows indicate the ventral hypothalamic midline. (A-D,F,G) Coronal sections with dorsal towards the top. (E,H) Horizontal sections with posterior towards the top. cc, cerebral cortex; vtel, ventral telencephalon. Scale bars: 200 μm in A,C,E; 50 μm in B,D,F-H.

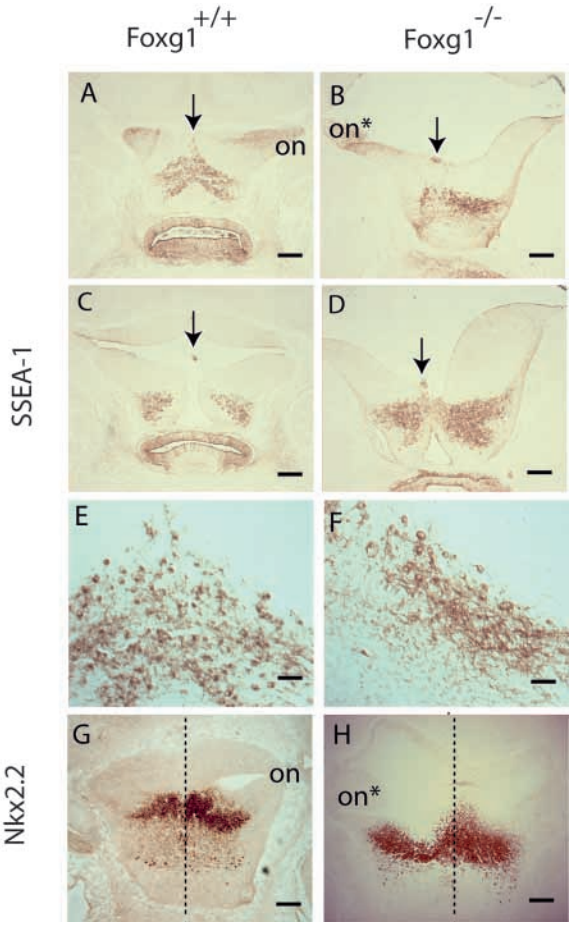

Fig. 7. Patterning of the chiasm at E13.5. Sections are horizontal, anterior is upwards. Immunohistochemistry was performed using antibodies for SSEA-1 (A-F) and Nkx2.2 (G,H). (A) Wild-type section through the optic chiasm showing SSEA-1-positive neurons arrayed in an inverted 'V'-shape. Arrow indicates the tip of the 'V'. SSEA-1 expression is also evident in the optic nerves (on). (B) A *Foxg1*$^{-/-}$ section equivalent to (A) showing SSEA-1 expression in the mutant correlate of the optic nerve (on*). Note that the plane of section is slightly tilted such that the left side is ventral to the right. The SSEA-1-positive 'arm' of the 'V' is visible on the right side, but is less clear on the left, which is further ventral. (C,D) Immediately dorsal to the optic chiasm, wild-type and *Foxg1*$^{-/-}$ embryos show bilaterally symmetrical SSEA-1 expression posterior to the third ventricle. SSEA-1 expression extends posteriorly and laterally in both C and D. (E,F) High magnification showing the morphology of SSEA-1 neurons in the wild type and *Foxg1*$^{-/-}$ mutant. (G,H) In the wild type and *Foxg1*$^{-/-}$ mutant, Nkx2.2 is expressed at the posterior optic chiasm, where it overlaps partly with SSEA-1 expression. Broken lines indicate the position of the midline. Scale bar: 200 μm in A,B; 100 μm in C,D,G,H; 50 μm in E,F.

both nasally and temporally. Given the expression patterns discussed above, abnormal development of RGC axons from both nasal and temporal territories argues against a completely cell-autonomous role for Foxg1 in the control of RGC projections. Foxg1 may autonomously regulate the behaviour of nasal RGC growth cones at the optic chiasm, e.g. by influencing their expression of cell surface molecules, but this can not be the case for most temporal RGCs.

The eyes of mice lacking Foxg1 have an abnormal shape (Xuan et al., 1995; Huh et al., 1999) (present study). A striking feature of the *Foxg1*$^{-/-}$ phenotype is the lack of an optic stalk connecting the retina to the brain. This could result in the retina becoming stretched medially as the head grows. Consistent with this, the overall volume and patterning of gene expression along its nasotemporal and dorsoventral axes are similar to wild-type retina. This argues against a fundamental repatterning of the retina in the absence of Foxg1. Changes in *Foxg1*$^{-/-}$ retinal morphology might also be secondary to defective development of the lens, which expresses Foxg1 early in its formation and is smaller than normal in mutants (Figs 2, 5) (Hatini et al., 1994; Xuan et al., 1995; Dou et al., 1999; Huh et al., 1999). Previous studies have shown that, although lens is not necessary to instruct the differentiation of neuroretina, it does influence the morphology of the retina either mechanically or molecularly (Ashery-Padan et al., 2000).

Foxg1 can be added to the growing list of proteins with a dual role in tissue morphogenesis and axon growth and morphology. Others on this list include transcription factors such as Pax6 (Ericson et al., 1997; Mastick et al., 1997; Pratt et al., 2000; Pratt et al., 2002) and secreted proteins of the Wnt (Hall et al., 2000; Yoshikawa et al., 2003), bone morphogenetic protein (BMP) (Augsburger et al., 1999) and hedgehog (Charron et al., 2003) families. Enzymes involved in regulating the sulphation status of extracellular heparan sulphate proteoglycans are implicated in Shh, Wnt and BMP signalling, tissue morphogenesis (Merry and Wilson, 2002; McLaughlin et al., 2003a) and RGC axon guidance (Walz et al., 1997; Irie et al., 2002).

Foxg1 may act at the optic chiasm to control RGC growth cone navigation

The simplest explanation of our finding an increased ipsilateral projection in embryos lacking Foxg1 is that Foxg1 normally regulates the proportions of crossed and uncrossed projections by a direct action on both temporal and nasal axons at the chiasm itself. In the chick, Foxg1 has been shown to autonomously regulate the retinotectal mapping of RGC axons (Yuasa et al., 1996) and it is possible that in the mouse Foxg1 expression by RGCs is involved in retinotectal mapping rather than in regulating midline crossing at the optic chiasm.

In the wild-type the diencephalon is surrounded on each side by a large telencephalic vesicle. This physical support is missing in the mutant, which has a hypoplastic telencephalon and, as a consequence, the diencephalon adopts a more 'open' conformation. Nevertheless, we found that many morphological and molecular features of the wild-type chiasm were retained in the mutant. The normal developing chiasm has been characterised in terms of the expression of transcription factors and regulatory molecules whose expression domains coincide with navigating RGC axons (Marcus et al., 1999; Nakagawa et al., 2000; Williams et al., 2003). We did not detect any gross abnormalities in the distribution of cells expressing the transcription factors Foxg1 or Nkx2.2 or of cells expressing cell surface molecules SSEA-1 or ephrin B2 at the developing chiasm. Despite its elongated shape, the mutant eye projects a correlate of the optic nerve, which converges to form the optic chiasm. It is extremely unlikely that anatomical alterations of the mutant eye or brain are solely responsible for the alterations

in the balance of ipsilateral and contralateral projections. Taken together, these findings point to a more specific defect causing the change in RGC axon midline crossing in mutants.

The mechanisms that regulate RGC growth cone navigation at the normal optic chiasm are not well understood, although it is known that Ephb and ephrin B family members are likely to participate in regulating midline crossing of RGC growth cones (Nakagawa et al., 2000; Barbieri et al., 2002; Williams et al., 2003). We did not detect obvious alterations in the distributions of Ephb2 and ephrin B2 protein in the mutant retina and optic chiasm but this does not necessarily preclude a role for Foxg1 in the control of Ephb/ephrin B signalling. There are several precedents for a particular receptor/ligand interaction leading to either attraction or repulsion depending on other factors. The presence of the extracellular matrix molecule laminin has been shown to convert the attraction of RGC growth cones towards a source of netrin to a repulsion of RGC growth cones away from a source of netrin (Hopker et al., 1999). Levels of an intracellular guanylate cyclase control the response of neocortical growth cones to a Sema3a gradient (Polleux et al., 2000). Although an analagous mechanism has not been demonstrated for Ephb/ephrin B signalling it appears that Ephb-expressing axons can be either attracted or repelled by ephrin B in different situations (McLaughlin et al., 2003b; Hindges et al., 2002).

Foxg1 may, therefore, regulate expression at the optic chiasm of one or more of a potentially very large number of modulators of signalling pathways activated by, for example, Ephb/ephrin B. The identification of transcriptional targets of Foxg1 will allow a systematic survey of these possibilities. The final choice made by each RGC growth cone whether to go ipsilateral or contralateral at the optic chiasm probably depends on the balance between attractive and repulsive signals at the chiasm and the nature of the response of each growth cone to those signals. Most probably loss of Foxg1 promotes ipsilateral projections at the optic chiasm by perturbing these balances.

We thank Katy Gillies, Ben Martynoga, James O'Connor, Duncan Mcneil and Linda Wilson (Biomedical Sciences Confocal Facility) for their contribution to this work. We thank Lijian Shen and Eseng Lai for providing the *Foxg1^{lacZ}* mice, and Jean Hebert and Susan McConnell for providing the *Foxg1^{Cre}* mice. The Nkx2.2 (74.5A5) and Ssea1 (MC-480) antibodies developed by Thomas Jessell and Davor Solter, respectively, were obtained from the Developmental Studies Hybridoma Bank developed under the auspices of the NICHD and maintained by The University of Iowa, Department of Biological Sciences, Iowa City, IA 52242. This work was supported by the Wellcome Trust, MRC and BBSRC.

References

Ashery-Padan, R., Marquardt, T., Zhou, X. and Gruss, P. (2000). Pax6 activity in the lens primordium is required for lens formation and for correct placement of a single retina in the eye. *Genes Dev.* **14**, 2701-2711.

Augsburger, A., Schuchardt, A., Hoskins, S., Dodd, J. and Butler, S. (1999). BMPs as mediators of roof plate repulsion of commissural neurons. *Neuron* **24**, 127-141.

Barbieri, A. M., Broccoli, V., Bovolenta, P., Alfano, G., Marchitiello, A., Mocchetti, C., Crippa, L., Bulfone, A., Marigo, V., Ballabio, A. et al. (2002). Vax2 inactivation in mouse determines alteration of the eye dorsal-ventral axis, misrouting of the optic fibres and eye coloboma. *Development* **129**, 805-813.

Batlle, E., Henderson, J. T., Beghtel, H., van den Born, M. M., Sancho, E., Huls, G., Meeldijk, J., Robertson, J., van de Wetering, M., Pawson, T. et al. (2002). Beta-catenin and TCF mediate cell positioning in the intestinal epithelium by controlling the expression of EphB/ephrinB. *Cell* **111**, 251-263.

Charron, F., Stein, E., Jeong, J., McMahon, A. P. and Tessier-Lavigne, M. (2003). The morphogen sonic hedgehog is an axonal chemoattractant that collaborates with netrin-1 in midline axon guidance. *Cell* **113**, 11-23.

Colello, R. J. and Guillery, R. W. (1990). The early development of retinal ganglion cells with uncrossed axons in the mouse: retinal position and axonal course. *Development* **108**, 515-523.

de Melo, J., Qiu, X., Du, G., Cristante, L. and Eisenstat, D. D. (2003). Dlx1, Dlx2, Pax6, Brn3b, and Chx10 homeobox gene expression defines the retinal ganglion and inner nuclear layers of the developing and adult mouse retina. *J. Comp. Neurol.* **461**, 187-204.

Dou, C. L., Li, S. and Lai, E. (1999). Dual role of brain factor-1 in regulating growth and patterning of the cerebral hemispheres. *Cereb. Cortex* **9**, 543-550.

Drager, U. C. (1985). Birth dates of retinal ganglion cells giving rise to the crossed and uncrossed optic projections in the mouse. *Proc. R. Soc. London B. Biol. Sci.* **224**, 57-77.

Ericson, J., Rashbass, P., Schedl, A., Brenner-Morton, S., Kawakami, A., van Heyningen, V., Jessell, T. M. and Briscoe, J. (1997). Pax6 controls progenitor cell identity and neuronal fate in response to graded Shh signaling. *Cell* **90**, 169-180.

Hall, A. C., Lucas, F. R. and Salinas, P. C. (2000). Axonal remodeling and synaptic differentiation in the cerebellum is regulated by WNT-7a signaling. *Cell* **100**, 525-535.

Hallonet, M., Hollemann, T., Pieler, T. and Gruss, P. (1999). Vax1, a novel homeobox-containing gene, directs development of the basal forebrain and visual system. *Genes Dev.* **13**, 3106-3114.

Hatini, V., Tao, W. and Lai, E. (1994). Expression of winged helix genes, BF-1 and BF-2, defines adjacent domains within the developing forebrain and retina. *Neurobiology* **25**, 1293-1309.

Hébert, J. M. and McConnell, S. K. (2000). Targeted introduction of *Cre* into the *Foxg1* (*BF-1*) locus mediates *loxP* recombination in the telencephalon and other developing head structures. *Dev. Biol.* **222**, 296-306.

Herrera, E., Brown, L., Aruga, J., Rachel, R. A., Dolen, G., Mikoshiba, K., Brown, S. and Mason, C. A. (2003). Zic2 patterns binocular vision by specifying the uncrossed retinal projection. *Cell* **114**, 545-557.

Hindges, R., McLaughlin, T., Genoud, N., Henkemeyer, M. and O'Leary, D. D. (2002). EphB forward signaling controls directional branch extension and arborization required for dorsal-ventral retinotopic mapping. *Neuron* **35**, 475-487.

Hopker, V. H., Shewan, D., Tessier-Lavigne, M., Poo, M. and Holt, C. (1999). Growth-cone attraction to netrin-1 is converted to repulsion by laminin-1. *Nature* **401**, 69-73.

Huh, S., Hatini, V., Marcus, R. C., Li, S. C. and Lai, E. (1999). Dorsal-ventral patterning defects in the eye of BF-1-deficient mice associated with a restricted loss of shh expression. *Dev. Biol.* **211**, 53-63.

Irie, A., Yates, E. A., Turnbull, J. E. and Holt, C. E. (2002). Specific heparan sulfate structures involved in retinal axon targeting. *Development* **129**, 61-70.

Mao, X., Fujiwara, Y. and Orkin, S. H. (1999). Improved reporter strain for monitoring Cre recombinase-mediated DNA excisions in mice. *Proc. Natl. Acad. Sci. USA* **96**, 5037-5042.

Marcus, R. C. and Mason, C. A. (1995). The first retinal axon growth in the mouse optic chiasm: axon patterning and the cellular environment. *J. Neurosci.* **15**, 6389-6402.

Marcus, R. C., Blazeski, R., Godement, P. and Mason, C. A. (1995). Retinal axon divergence in the optic chiasm: uncrossed axons diverge from crossed axons within a midline glial specialisation. *J. Neurosci.* **15**, 3716-3729.

Marcus, R. C., Shimamura, K., Sretavan, D., Lai, E., Rubenstein, J. L. R. and Mason, C. A. (1999). Domains of regulatory gene expression and the developing optic chiasm: correspondence with retinal axon paths and candidate signaling cells. *J. Comp. Neurol.* **403**, 346-358.

Mastick, G. S., Davis, N. M., Andrew, G. L. and Easter, S. S., Jr (1997). Pax-6 functions in boundary formation and axon guidance in the embryonic mouse forebrain. *Development* **124**, 1985-1997.

McLaughlin, D., Karlsson, F., Tian, N., Pratt, T., Bullock, S. L., Wilson, V. A., Price, D. J. and Mason, J. O. (2003a). Specific modification of heparan sulphate is required for normal cerebral cortical development. *Mech. Dev.* **120**, 1481-1488.

McLaughlin, T., Hindges, R., Yates, P. A. and O'Leary, D. D. (2003b). Bifunctional action of ephrin-B1 as a repellent and attractant to control

bidirectional branch extension in dorsal-ventral retinotopic mapping. *Development* **130**, 2407-2418.

Merry, C. L. and Wilson, V. A. (2002). Role of heparan sulfate-2-O-sulfotransferase in the mouse. *Biochim. Biophys. Acta* **157**, 319-327.

Mui, S. H., Hindges, R., O'Leary, D. D., Lemke, G. and Bertuzzi, S. (2002). The homeodomain protein Vax2 patterns the dorsoventral and nasotemporal axes of the eye. *Development* **129**, 797-804.

Nakagawa, S., Brennan, C., Johnson, K. G., Shewan, D., Harris, W. A. and Holt, C. E. (2000). Ephrin-B regulates the Ipsilateral routing of retinal axons at the optic chiasm. *Neuron* **25**, 599-610.

Perron, M., Kanekar, S., Vetter, M. L. and Harris, W. A. (1998). The genetic sequence of retinal development in the ciliary margin of the *Xenopus* eye. *Dev. Biol.* **199**, 185-200.

Polleux, F., Morrow, T. and Ghosh, A. (2000). Semaphorin 3A is a chemoattractant for cortical apical dendrites. *Nature* **404**, 567-573.

Pratt, T., Vitalis, T., Warren, N., Edgar, J. M., Mason, J. O. and Price, D. J. (2000). A role for Pax6 in the normal development of dorsal thalamus and its cortical connections. *Development* **127**, 5167-5178.

Pratt, T., Quinn, J. C., Simpson, T. I., West, J. D., Mason, J. O. and Price, D. J. (2002). Disruption of early events in thalamocortical tract formation in mice lacking the transcription factors Pax6 or Foxg1. *J. Neurosci.* **22**, 8523-8531.

Reese, B. E., Necessary, B. D., Tam, P. P. L., Faulkner-Jones, B. and Tan, S.-S. (1999). Clonal expansion and cell dispersion in the developing mouse retina. *Eur. J. Neurosci.* **11**, 2965-2978.

Rubenstein, J. L. and Beachy, P. A. (1998). Patterning of the embryonic forebrain. *Curr. Opin. Neurobiol.* **8**, 18-26.

Rubenstein, J. L., Shimamura, K., Martinez, S. and Puelles, L. (1998). Regionalization of the prosencephalic neural plate. *Annu. Rev. Neurosci.* **21**, 445-477.

Sretavan, D. W. and Reichardt, L. F. (1993). Time-lapse video analysis of retinal ganglion cell axon pathfinding at the mammalian optic chiasm: growth cone guidance using intrinsic chiasm cues. *Neuron* **10**, 761-777.

Sretavan, D. W., Feng, L., Pure, E. and Reichardt, L. F. (1994). Embryonic neurons of the developing optic chiasm express L1 and CD44, cell surface molecules with opposing effects on retinal axon growth. *Neuron* **12**, 957-975.

Sretavan, D. W., Pure, E., Siegel, M. W. and Reichardt, L. F. (1995). Disruption of retinal axon ingrowth by ablation of embryonic mouse optic chiasm neurons. *Science* **269**, 98-101.

Torres, M., Gomez-Pardo, E. and Gruss, P. (1996). Pax2 contributes to inner ear patterning and optic nerve trajectory. *Development* **122**, 3381-3391.

Walz, A., McFarlane, S., Brickman, Y. G., Nurcombe, V., Bartlett, P. F. and Holt, C. E. (1997). Essential role of heparan sulfates in axon navigation and targeting in the developing visual system. *Development* **124**, 2421-2430.

Wang, S. W., Mu, X., Bowers, W. J., Kim, D. S., Plas, D. J., Crair, M. C., Federoff, H. J., Gan, L. and Klein, W. H. (2002). Brn3b/Brn3c double knockout mice reveal an unsuspected role for Brn3c in retinal ganglion cell axon outgrowth. *Development* **129**, 467-477.

Williams, S. E., Mann, F., Erskine, L., Sakurai, T., Wei, S., Rossi, D. J., Gale, N. W., Holt, C. E., Mason, C. A. and Henkemeyer, M. (2003). Ephrin-B2 and EphB1 mediate retinal axon divergence at the optic chiasm. *Neuron* **39**, 919-935.

Wizenmann, A., Thanos, S., von Boxberg, Y. and Bonhoeffer, F. (1993). Differential reaction of crossing and non-crossing rat retinal axons on cell membrane preparations from the chiasm midline: an in vitro study. *Development* **117**, 725-735.

Xuan, S., Baptista, C. A., Balas, G., Tao, W., Soares, V. C. and Lai, E. (1995). Winged helix transcription factor BF-1 is essential for the development of the cerebral hemispheres. *Neuron* **14**, 1141-1152.

Yoshikawa, S., McKinnon, R. D., Kokel, M. and Thomas, J. B. (2003). Wnt-mediated axon guidance via the *Drosophila* derailed receptor. *Nature* **422**, 583-588.

Yuasa, J., Hirano, S., Yamagata, M. and Noda, M. (1996). Visual projection map specified by topographic expression of transcription factors in the retina. *Nature* **382**, 632-635.

Zuber, M. E., Gestri, G., Viczian, A. S., Barsacchi, G. and Harris, W. A. (2003). Specification of the vertebrate eye by a network of eye field transcription factors. *Development* **130**, 5155-5167.